# Towards Thermodynamics of Spatiotemporal Chaos

Kunihiko KANEKO

*Institute of Physics, College of Arts and Sciences*
*University of Tokyo, Komaba, Tokyo 153*

Thermodynamics of spatiotemporal chaos is discussed, with the use of coupled map lattices. Structural stability of fully developed spatiotemporal chaos (FDSTC) is confirmed. The stability is sustained by the destruction of all windows through spatiotemporal intermittency and supertransients. In FDSTC, spatial and temporal correlations are found to decay exponentially, as are measured by mutual information. The existence of finite correlation length assures the density of thermodynamic quantifiers. In FDSTC, it is possible to obtain the thermodynamical densities only from measurement within a subspace. On this purpose, subspace Lyapunov spectra are introduced. Only from data of the dynamics within a subspace, thermodynamic quantifiers such as Kolmogorov-Sinai entropy density, Lyapunov dimension density, and scaled Lyapunov spectra are estimated. Application of this approach to the diagnosis of experimental data of spatially extended systems is proposed. To study the fluctuation of Lyapunov spectrum, sub-spacetime Lyapunov exponent is introduced. It provides a way to distinguish chaotic region from ordered region in spacetime. Distribution of sub-spacetime Lyapunov exponents is calculated which characterizes the change of pattern dynamics clearly. As a theoretical approach to spatiotemporal chaos, self-consistent Perron-Frobenius operator is introduced. The invariant measure in a subspace is obtained as the fixed point function for this operator. Some applications to spatiotemporal intermittency transitions and pattern dynamics are presented.

## Contents

§ 1. Introduction
§ 2. Stability of fully developed spatiotemporal chaos : destruction of windows and spatiotemporal intermittency
Fully developed spatiotemporal chaos
Destruction of windows : spatiotemporal intermittency
Destruction of windows: spatiotemporal intermittency and supertransient turbulence
§ 3. Mutual information
§ 4. Subspace Lyapunov spectrum
§ 5. Possible diagnosis of experimental data
§ 6. Sub-spacetime Lyapunov exponent
§ 7. Self-consistent Perron-Frobenius operator
§ 8. Summary and discussion
References

## § 1. Introduction

Spatiotemporal chaos is complex dynamical phenomenon with many degrees of freedom, emerging in spatially extended systems. It appears in a broad area of natural phenomena, including fluid turbulence, chemical turbulence, solid state physics such as Josephson junction array, charge density wave, and spin density wave, liquid crystal convection, biological information processing, and so on. Qualitative, quantitative and theoretical understanding of spatiotemporal chaos remains one of the most important problems in nonlinear dynamics.

As a simple model for spatiotemporal chaos, coupled map lattices (CML) have been proposed.[1)~3)] Studies of spatiotemporal chaos by CML have been growing rapidly within these few years.[4)~18)]

A CML is a dynamical system with a discrete time, discrete space, and continuous state.[1)~12)] Although there are various kinds of couplings between nearby lattice points which may be used in a CML, we restrict ourselves here to the following diffusive coupling case here:

$$x_{n+1}(i)=(1-\epsilon)f(x_n(i))+\epsilon/2[f(x_n(i+1))+f(x_n(i-1))]\,, \tag{1}$$

where $n$ is a discrete time step and $i$ is a lattice point ($i=1, 2, \cdots, N=$system size) with a periodic boundary condition. Here the mapping function $f(x)$ is chosen to be the logistic map $f(x)=1-ax^2$ (coupled logistic lattice). Results to be presented here are applied to other maps and couplings.

Separation of procedures is important in the construction of CML. In the above model, local nonlinear transformation and diffusion process are separated: The dynamics consists of $x_n(i)\to x'(i)=f(x_n(i))$ and then the discrete Laplacian operator $x_{n+1}(i)=(1-\epsilon)x'(i)+(\epsilon/2)(x'(i+1)+x'(i-1))$. As has been discussed, this separation of procedures is essential to the modelling.[1),5),13)]

Merits of CML are as follows: (i) It is numerically efficient, since it is semi-coarse-grained description: (ii) Dynamical systems theory and quantification of low-dimensional chaos are extended to include spatial degrees of freedom: (iii) Statistical mechanical treatment is possible: (iv) It captures the essence of spatiotemporal chaos.

The original motivation of the introduction of CML has been to understand turbulent behavior as (hyper)$^\infty$ chaos. In other words, it is invented in the endeavor towards the synthesis of Landau's picture on turbulence[22)] and Rössler's hyperchaos.[24)] Landau regarded turbulence as a direct product of periodic states (that is a quasiperiodic state with many incommensurate frequencies). Unfortunately, this direct product state is unstable, and is easily locked to a lower-dimensional torus,[2)] or attracted to a nearby strange attractor.[23),2)] On the other hand, it may be possible to construct a turbulence model as a direct product of chaos ((hyper)$^\infty$ chaos), if it is stable. For this motivation, CML has originally been introduced.[1),2)]

Not only Landau's high-dimensional quasiperiodic state but also low-dimensional chaotic state is structurally unstable. In the logistic map, for example, chaos cannot

exist in an open set in the parameter space. Periodic windows are dense, although the chaotic state also has positive measure in the parameter space. Quantifiers such as Lyapunov exponent, have infinitely many drops, if plotted as a function of bifurcation parameter. Chaotic state is structurally unstable, even if it is observable.

As will be seen in § 2, fully developed chaotic state in our model is structurally stable. All windows are destroyed for almost all initial conditions. Mechanism of this destruction turns out to be spatiotemporal intermittency[1),4),5),9)] and super-transients.[10)]

In fully developed spatiotemporal chaos, spatial correlation decays exponentially. Then, two points distant farther than the correlation length $\xi$ move independently. Our system is roughly approximated by a direct product of $(N/\xi)$ independent systems. Then the number of positive Lyapunov exponents, Kolomogov-Sinai entropy and the dimension of attractors are expected to be proportional to the system size $N$.[3),4),12)] This existence of extensive quantifiers assures well-defined existence of thermodynamic densities, as is discussed in § 3.

If such densities exist, it is expected that the information of thermodynamic quantities can be obtained only from the data in subspace. On this purpose, subspace Lyapunov spectra are introduced in § 4. Only from the timeseries within a small subspace, one can estimate the thermodynamic densities of the total system. Application of this method to experimental data is discussed in § 5.

By extending this method to subspace and sub-time (finite time), it is possible to quantify the strength of chaos in spacetime. Application of sub-spacetime Lyapunov exponents to spatiotemporal intermittency will be discussed in § 6. Fluctuation of Lyapunov exponents in spacetime is obtained from the distribution of sub-spacetime Lyapunov exponents. Based on this distribution, one can expect the statistical treatment analogous to the large deviation theory of low-dimensional chaos.

In fully developed spatiotemporal chaos, we can expect the construction of statistical mechanics. Through the statistical mechanical formulation, we may relate various thermodynamic quantifiers with each other. As a simple step towards a theoretical formulation, a self-consistent Perron-Frobenius operator is introduced.[13)] Application to spatiotemporal intermittency is discussed in § 7.

## § 2. Stability of fully developed spatiotemporal chaos : destruction of windows and spatiotemporal intermittency

*Fully developed spatiotemporal chaos*

As has been investigated in detail,[1),4),5)] our CML exhibits the following phase changes: (i) periodic states with kinks, (ii) frozen random pattern with localized chaos, (iii) pattern selection, (iv) spatiotemporal intermittency transition and (v) fully developed spatiotemporal chaos (FDSTC).

In FDSTC, all quantifiers change smoothly with parameters for almost all initial conditions. In Fig. 1, we have plotted Kolmogorov-Sinai entropy and maximal Lyapunov exponent as a function of bifurcation parameter $a$.

Figure 1 is in strong contrast with the graph for the bifurcation in the single

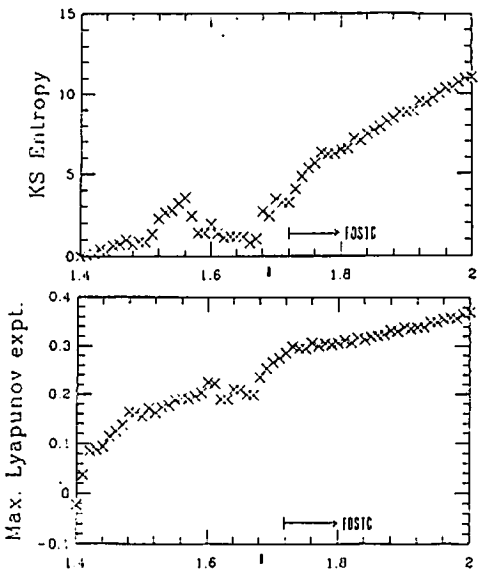


Fig. 1. Kolmogorov-Sinai entropy (a) and maximal Lyapunov exponent (b) of our logistic lattice (1), as a function of $a$, calculated from the Lyapunov spectra (see § 4 for details). The spectra are obtained from 3000 steps after discarding 2000 transients, starting from a random initial condition. $\epsilon=.2$ and $N=64$.

logistic map. In the logistic map, periodic windows are dense. Both chaos and periodic windows have positive measure in the parameter space. Chaos cannot exist in an open set in the parameter space. Lyapunov exponent, therefore has infinitely many drops, if plotted as a function of bifurcation parameter. Chaotic state is structurally unstable, even if it has a positive measure in the parameter space.

On the other hand, our FDSTC seems to be structurally stable for almost all initial conditions. We have not observed any windows in the parameter regimes for FDSTC, if we start from randomly chosen initial conditions.

*Destruction of windows: spatiotemporal intermittency*

Why do windows in the logistic map disappear in coupled systems? If $x=x_j^*(j=1, 2, \cdots, p)$ is a stable cycle of the period $p$ for the logistic map in a window, spatially homogeneous and temporally periodic state $x(i)=x_j^*$ is linearly stable, as can be easily checked. This window should be observed for initial conditions in the vicinity of the homogeneous state. For most initial conditions, however, windows are not observed. This means that we have to investigate the basin volume of such homogeneous attractor, and the transient time before our system is attracted into the homogeneous attractor.

As a simple example, let us consider the period-3 window in the logistic map. Period-3 cycle is stable for $1.75<a<1.76\cdots$ for logistic map. In Fig. 2, $f^3(x)$ is plotted. We have three stable fixed points $x_1^*$, $x_2^*$, $x_3^*$ of $f^3(x)$ corresponding to the period-3 cycle in the logistic map. In our logistic lattice the homogeneous period-3 state ($x(i)=x_m^*$) is stable for this parameter range. However, the basin volume ratio for such homogeneous state is extremely small.*) We have never encountered with the attraction into this homogeneous state, as far as we take arbitrarily chosen initial conditions.

The homogeneous period-3 state has basin of attraction only in the vicinity of such homogeneous initial conditions. Let us denote the unstable period-3 cycle by $x_1'$, $x_2'$ and $x_3'$ (in other words the unstable fixed points of $f^3(x)$) and introduce the interval $I_j$ as $I_j\equiv[x_j^*, x_j']$ (see Fig. 2). Define an initial condition curve $x_0(r)$ as a piecewise-linear connection of $x_0(i)$ (i.e., $x_0(r)=x_0(j)+(x_0(j+1)-x_0(j))\times(r-j)$ for $j\le r\le j+1$).

*) Here the "basin" for a given state means the set of initial conditions which are attracted to the state within a non-astronomical time, that is less than the order of $\exp(\text{const}\times N)$.

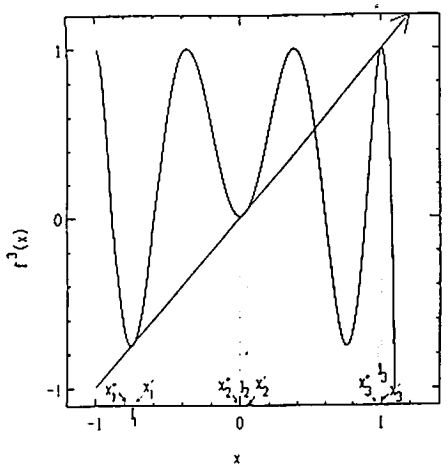


Fig. 2. $f^3(x)$ of the single logistic map. $a=1.752$. If the initial value of $x$ lies in $I_i$, $x_n$ is attracted to $x_i^*$, a fixed point of $f^3(x)$, without any chaotic transients. Still there is topological chaos; chaotic motion exists on a Cantor set between $I_i$ and $I_k$. The existence of topological chaos without chaotic attractor in the local map is necessary to create the spatiotemporal intermittency in a coupled system.

If $x_0(r)$ is confined in a unique $I_k$ initially (in other words, all of the $x_0(i)$'s belong to a unique interval $I_k$), our lattice is attracted to the homogeneous cycle within non-astronomical time steps. On the other hand, if an initial condition $x_0(r)$ covers at least two intervals $I_i$ and $I_j$ $(j\neq i)$, it is not attracted into the homogeneous state within non-astronomical time steps. For such an initial condition there are lattice points which take a value between $I_i$ and $I_j$. The local dynamics of logistic map gives transient chaos at this range of value. The lattice point should move chaotically in time. If the coupling is not extremely small (typically larger than the order of 0.001), this chaotic region propagates to neighboring lattice points. See Figs. 4 and 6 of Ref. 1b) for the propagation of the chaos by this machanism. This mechanism is called spatiotemporal intermittency.[1,41,9] Thus we can say that windows in local dynamics are extinguished by spatiotemporal intermittency for a coupled system. This is why all physical quantities change smoothly with a parameter in FDSTC.

The volume ratio of the condition with $\forall x_0(i)\in$unique $I_j$ decreases exponentially with the system size $N$. Thus the probability to hit the homogeneous attractor goes to zero with the increase of system size.

We note that topological chaos is essential to spatiotemporal intermittency. If there is no topological chaos in the local dynamics, the above argument does not hold. Indeed, a cycle with period $2^n$ is stable with kinks.[1] Since there is no topologial chaos in the parameter regime for period $2^n$ in the logistic map, the kink dynamics between the values of $I_i$ and $I_j$ does not exhibit any chaotic behavior. Kinks are thus stabilized and pinned at its position.

To sum up, *Coupling periodic local dynamics with TOPOLOGICAL CHAOS induces spatiotemporal intermittency.*

In a one-dimensional map, Li and Yorke have proved the famous phrase "Period three implies chaos".[25] Since the chaos in their proof is topological chaos, but not necessarily observable chaos, this phrase is not always valid to observable (physical) chaos. On the other hand, we can conclude the following statement on spatiotemporal chaos, by combining the above summary with Li-Yorke's phrase: "Coupled period-3 implies observable spatiotemporal chaos".

*Destruction of windows: spatiotemporal intermittency and supertransient turbulence*

Here we show that spatiotemporal intermittency is not the final attractor but

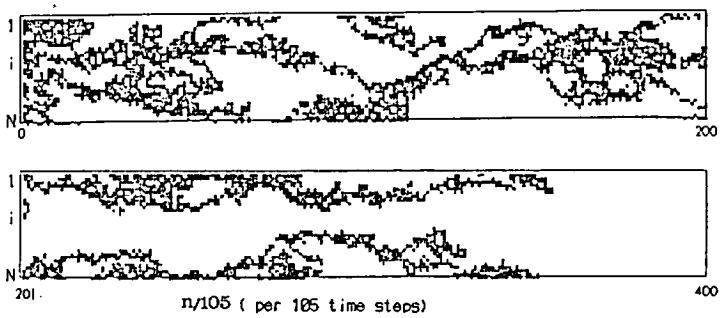


Fig. 3. Spatial derivative plots for the coupled logistic lattice (1), with $\epsilon=0.001$, $N=30$ and starting with a random initial condition. Every 105th step is plotted. If $|x_n(i+1)-x_n(i)|$ is larger than .3, the corresponding spacetime pixel is painted as black, painted as gray if it is between .1 and .3, while it is left blank otherwise. Around the time step 36000, intermittent transients disappear and our system is attracted into the homogeneous period-3 cycle.

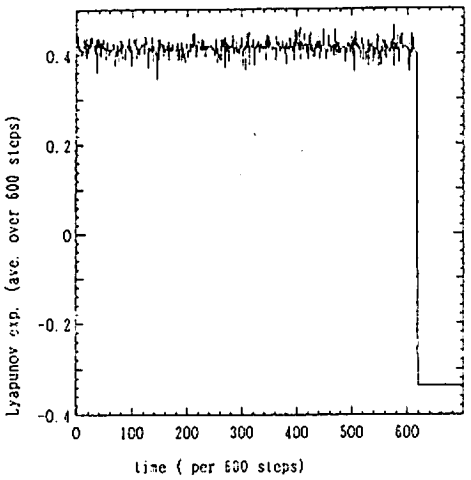


Fig. 4. Short-time Lyapunov exponent of our logistic lattice (1), plotted as a function of time. Using the $N$-dimensional Jacobi matrix $J$ of our lattice dynamics, short-time Lyapunov exponent $\lambda(t)$ is defined by the logarithm of the largest eigenvalue of $\Pi_{t=1}^{M}J_{M(t-1)}$. $M$ is chosen to be 600. $a=1.752$, $\epsilon=0.0011$, and $N=30$ and starting with a random initial condition.

type-II supertransient turbulence.

Type-II supertransient is found and defined by Crutchfield and the author.[10] Definition of type-II supertransient turbulence is as follows:(1) the length of transient time diverges with system size exponentially or faster; (2) in the transient time steps, the motion is chaotic with many positive Lyapunov exponents; (3) there exists quasi-stationary measure; no decay is observed in the transient regime, and the termination of transients is abrupt.

Let us study coupled logistic lattice (1) with $a=1.752$. At this parameter the attractor of the single logistic map is period-3 cycle. If the coupling is smaller than $\epsilon<\epsilon_c\approx 8\times 10^{-4}$, our CML is attracted into this period-3 state with kinks within few time steps. If $\epsilon>\epsilon_c$, our system exhibits spatiotemporal intermittency as is discussed in the previous subsection.*)

In Fig. 3, spacetime diagram for a small lattice is shown. After many time steps, our system is finally attracted into the homogeneous period-3 state if $\epsilon<\epsilon_c$. As shown in the figure, our system exhibits typical spatiotemporal intermittency in the transient time regime.[1),9)]

To show the existence of quasistationary measure and of the rapid escape to the periodic state, we have plotted short-time Lyapunov exponent as a function of time. The maximal Lyapunov exponent is calculated by the average over given $M$ time

*) To be precise, there is small parameter regime $\epsilon_c<\epsilon<\epsilon'_c$ of type-I supertransients. Details will be reported elsewhere.

steps, without taking $M\to\infty$ limit (see also § 4). In Fig. 4, we have chosen $M=600$ time steps. The existence of quasistationary measure and a very rapid escape is clearly seen. In the figure, spatiotemporal intermittency terminates around $620\times600$ time steps, and is attracted to the fatal attractor, period-3 cycle.

In Figs. 5(a)~(c), average transient time steps before our system is attracted into period-3 state are plotted as a function of system size $N$.

For $\epsilon>\epsilon_c$, the transient length increases with the system size as

$$T_N=\text{const}\times\exp(rN)\,. \tag{2}$$

Here the coefficient $r$ increases with $\epsilon$ as

$$r\propto(a-a_c)^{\gamma}\,. \tag{3}$$

The exponent $\gamma$ is related with the exponent for the correlation length. The exponential divergence of the transient length is understood as follows: If our system

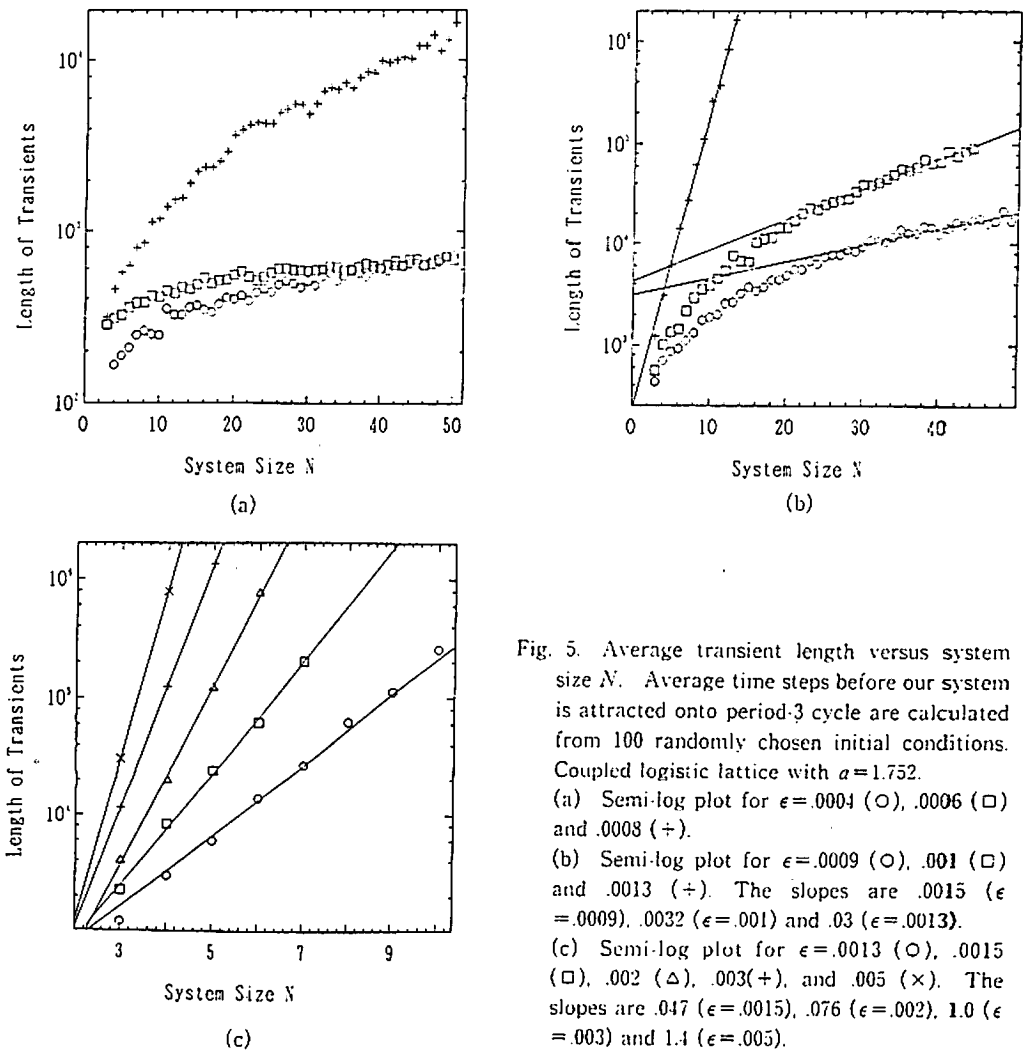


Fig. 5. Average transient length versus system size $N$. Average time steps before our system is attracted onto period-3 cycle are calculated from 100 randomly chosen initial conditions. Coupled logistic lattice with $a=1.752$.
(a) Semi-log plot for $\epsilon=.0004$ (○), .0006 (□) and .0008 (÷).
(b) Semi-log plot for $\epsilon=.0009$ (○), .001 (□) and .0013 (÷). The slopes are .0015 ($\epsilon=.0009$), .0032 ($\epsilon=.001$) and .03 ($\epsilon=.0013$).
(c) Semi-log plot for $\epsilon=.0013$ (○), .0015 (□), .002 (△), .003(+), and .005 (×). The slopes are .047 ($\epsilon=.0015$), .076 ($\epsilon=.002$), 1.0 ($\epsilon=.003$) and 1.4 ($\epsilon=.005$).

has a finite correlation length $\xi$, two elements distant farther than $\xi$ move essentially independently. Then our system is divided into $(N/\xi)$ subunits. As a simple approximation we can assume that each subunit takes either Laminar ($L$) or Turbulent ($T$) state. As long as there exists a turbulent site, it can propagate into neighboring sites. If all of our lattice points happen to hit Laminar state ($LLL\cdots LLL$), our system remains the $LLL\cdots LLL$ state. Thus the transient time before our system enters into the periodic state is approximated by the average waiting time before our system finds the $LLL\cdots LLL$ state. Using the single-point probability $p_L$ that an element takes Laminar state, and neglecting the correlation in neighboring subunits, the probability that all elements take $L$ is given by $(p_L)^{N/\xi}$. The average time to find the state $LLL\cdots LLL$ is inversely proportional to the above probability. Thus the transient length $T_N$ obeys

$$T_N \propto (p_L)^{-N/\xi} \propto \exp(\text{const} \times N/\xi). \tag{4}$$

If we follow the common sense of critical phenomena, the correlation length $\xi$ diverges as $\xi \propto (a-a_c)^{-\zeta}$. Our critical exponent $\gamma$ of transients is expected to be equal to the exponent $\zeta$.

Near $\epsilon \approx \epsilon_c$, transient length increases with some power; $T_N = N^\eta$. This power-law dependence is also expected from the power-law decay of correlation at the transition point.

## § 3. Mutual information

Chaotic dynamics exhibits the information flow in the bit space.[26] In spatiotemporal chaos, the information flows both in real and bit spaces. Mutual information is a powerful tool to measure the correlation and the information flow in spacetime. Here we use two-point mutual information flow in spacetime, to study the spatiotemporal correlation.*)

Let us introduce a single point distribution function $p(x(i))$ and two-point probability function $P(x_n(i), x_{n+t}(i+m))$. $p(x(i))$ is the probability function that the lattice site $i$ takes a value $x(i)$, while $P(x_n(i), x_{n+t}(i+m))$ is the probability that the lattice site $i$ takes a value $x_n(i)$ at time $n$ and the site $i+m$ takes $x_{n+t}(i+m)$ at time $n+t$. Mutual information between the two lattice points $i$ and $i+m$ is defined by[3]

$$I^{st}(t, m; i) = \int \log p(x(i))\, dx(i) + \int \log p(x(i+m))\, dx(i+m)$$
$$- \int \log P(x_n(i), x_{n+t}(i+m))\, dx_n(i)\, dx_{n+t}(i+m). \tag{5}$$

Temporal mutual information is the mutual information at the same lattice point with two different time steps $I^t(t; i) = I^{st}(t, 0; i)$. Spatial mutual information is that of two different lattice sites at the same time; $I^s(m; i) = I^{st}(0, m; i)$.

In numerical calculation of the probability function we have to use a finite bin

*) It is also important to introduce multi-point probability function and to study the cylinder entropy and spacetime patch entropy.

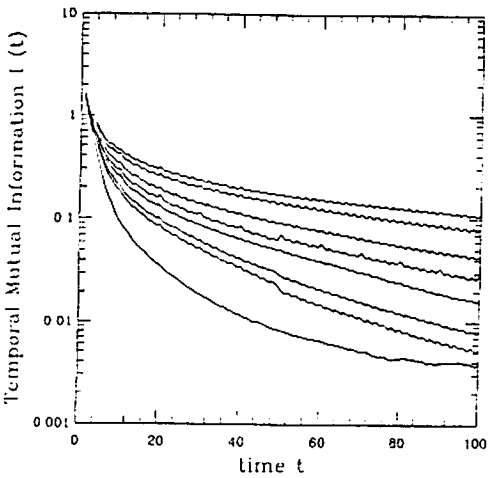


Fig. 6. Temporal mutual information flow for the logistic lattice (1): calculated using the bin number $M=64$ and 500000 time step sampling, after discarding 100000 step transients. $N=1000$, $\epsilon=.3$. $a=1.78$, 1.79, 1.8, 1.81, 1.82, 1.83, 1.84, and 1.88 from top to bottom. The site dependence is negligible here.

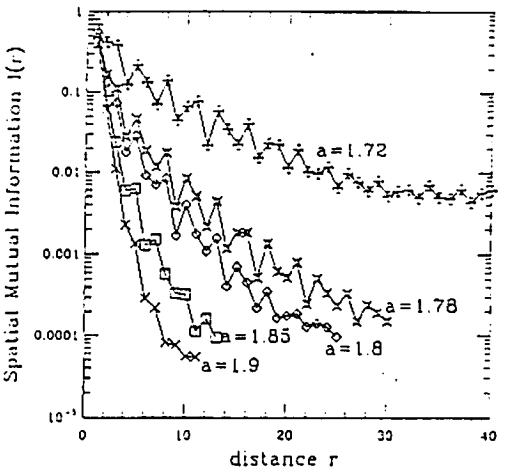


Fig. 7. Spatial mutual information flow for the logistic lattice (1), calculated in the same manner as Fig. 6. $\epsilon=3$, $M=32$, and $N=1000$. $a=1.72$, $a=1.78$, $a=1.8$, $a=1.85$ and $a=1.9$.

size, and replace the integral by the summation over bins. Taking the partition number $M$ for the interval $[-1, 1]$, the above probability functions are computed through the bins $[-1, -1+2/M]$, $[-1+2/M, -1+4/M]$, $\cdots$, $[-1+2n/M, -1+2(n+1)/M]$, $\cdots$, $[1-2/M, 1]$.*)

Temporal mutual information $I^t(t\,;\,i)$ for FDSTC is shown in Fig. 6. It decays exponentially with time. The function is independent of sites, showing the spatial ergodicity. These two features are in contrast with the results for the phases "Pattern Selection" and "Frozen Random Pattern".[4),15)] In these two phases, the decrease of mutual information stops at some value, and its functional form depends on sites.

The rate of the exponential decay decreases as the nonlinearity is decreased, till it goes to zero at the intermittency transition. The decay is roughly fitted by the power-law decay near the transition parameter.

Spatial mutual information is shown in Fig. 7. In FDSTC it decays exponentially with the distance $r$. The rate of decay decreases as the parameter approaches the transition point.

As is seen in Fig. 7, a smaller periodic modulation is added in the mutual information. It comes from the domain structure. Indeed, the domain size selected in the pattern selection phase has this wavelength. The above modulation shows the trace of this domain structure in the chaotic regime.

The mutual information with different time and space has originally been introduced in Ref. 3), as co-moving mutual information flow (COMIF). The mutual

*) Increase of the above mutual information with the partition number $M$ gives the rate of information creation. We can measure the spacetime flow of information creation. Although the creation rate is an important quantifier, we will not discuss it here. We fix $M=64$ throughout the paper.

information $I^{st}(t, t/v\,;\, i)$ with a given velocity $v$ quantifies the information propagation with the speed $v$. In soliton turbulence,[6] soliton-like excitations remain in turbulent states. In this case, COMIF $I^{st}(t, t/v\,;\, i)$ has a peak at a velocity of such soliton. In an open-flow problem,[7),3)] there exists propagation of kinks to downflow. COMIF has a sharp peak at the speed of kink. The peak decays slowly with time. This decay is originated in the chaotic interaction with other kinks.

## § 4. Subspace Lyapunov spectrum

Lyapunov spectra characterize how a small disturbance in tangential space is amplified or contracted. In an $N$-dimensional dynamical system, there are $N$ independent tangential vectors. Corresponding to them there exist $N$ eigenvalues, which form the spectrum.

In our CML, Lyapunov spectra can be defined by the product of Jacobi matrices. The logarithm of the eigenvalues of the product, divided by time steps $n$ with the limit $n\to\infty$ give Lyapunov exponents. The exponents $\lambda_i$ ordered from the largest to the smallest, give a spectrum. The maximal Lyapunov exponent $\lambda_1$ characterizes the rate how arbitrarily small disturbance is amplified. Sum of positive Lyapunov exponents give the amplification ratio of an $N$-dimensional tangential volume. It is equal to Kolmogorov-Sinai (KS) entropy which is originally defined as the increase rate of variety of symbol sequences.

Another useful quantity obtained from Lyapunov spectrum is Lyapunov dimension. It is defined by

$$D_L=j_p+\frac{\sum_{j=1}^{j_p}\lambda_j}{\lambda_{j+1}}, \tag{6}$$

where $j_p$ is the largest integer which satisfies $\sum_{j=1}^{j_p}\lambda_j>0$. According to Kaplan-Yorke formula,[27)] the Lyapunov dimension gives an estimate on the dimension of attractor.

As has already been discussed,[3)] the spectrum has a scaled form: $\lambda(x)\equiv\lambda_{Nx}$ converges to a single curve, independent of $N$, if $N$ is not too small. The existence of this scaled form assures the existence of Kolmogorov-Sinai entropy density $h\equiv(1/N)\sum_{j=1}^{j_p}\lambda_j$ and Lyapunov dimension density $d_L=[j_p+(\sum_{j=1}^{j_p}\lambda_j)/(\lambda_{j+1})]/N$.

A drawback in the study of these quantifiers lies in the necessity of long computation time. Although we can calculate the whole Lyapunov spectrum for CML within reasonable computational time, the calculation requires much longer time in PDE. In real experiments, it is practically impossible to get the spectrum if the system size and the dimension are large.

When the spatial correlation decays exponentially, two elements distant farther than the correlation length move essentially independently. It is expected that we can construct the thermodynamics of our whole system only from the information of a subsystem within the size of the order of the correlation length.

In the present section, we argue a possible way to reconstruct the whole Lyapunov spectrum from the measurement within a small subsystem. We introduce

the subspace Lyapunov spectrum here.*)

Take a subsystem $S[j, L]$, subspace consisting of sites $j$, $j+1$, $\cdots$, $j+L-1$, and define Lyapunov spectra at the subspace $S[j, L]$. We calculate how a tangential vector in this subspace $\delta x(j)$, $\delta x(j+1)$, $\cdots$, $\delta x(j+L-1)$ evolves. From the eigenspectrum of this evolution of tangential vectors, Lyapunov spectra are obtained, in the same manner as usual Lyapunov exponents. Here the amplification/contraction of small disturbances at the boundaries ($x(j-1)$ and $x(j+L)$) is neglected. Boundary effect comes in only through the motion of $x(j)$ and $x(j+L-1)$.

In our CML, the spectrum is calculated by the product of Jacobi matrices at site $j$,

$$J_n^{S[j,L]}{}_{i,k} \equiv (1-\epsilon) f'(x_n(i+j-1))\delta_{i,k} + (\epsilon/2)(f'(x_n(i+j))\delta_{i+1,k} + f'(x_n(i+j-2))\delta_{i-1,k}); \tag{7}$$

($\delta_{i,k}$ is Kronecker delta with $\delta_{0,0} \equiv \delta_{L+1,L+1} \equiv 0$). Logarithms of the eigenvalues of the product $\lim_{n\to\infty}(1/n)\log\prod_m^n J_m$ give the subspace Lyapunov spectrum.

Does the subspace Lyapunov spectrum give a good estimate for the whole spectrum? We can expect the affirmative answer if we adopt a heat-bath picture: Take a subsystem, and assume that the effect from other regions is replaced by a noise generated by spatiotemporal chaos.

In Fig. 8, scaled Lyapunov spectrum is plotted with the increase of subsystem size

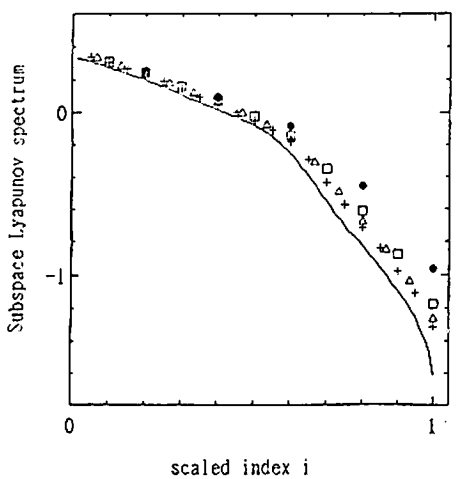


Fig. 8. Scaled Lyapunov spectra: Subspace Lyapunov spectra plotted for the subspace size 5 (•), 10 (□), 15 (△) and 20 (+). The curve shows the Lyapunov spectrum for the entire lattice. $a=1.9$, $\epsilon=.4$ and $N=100$.

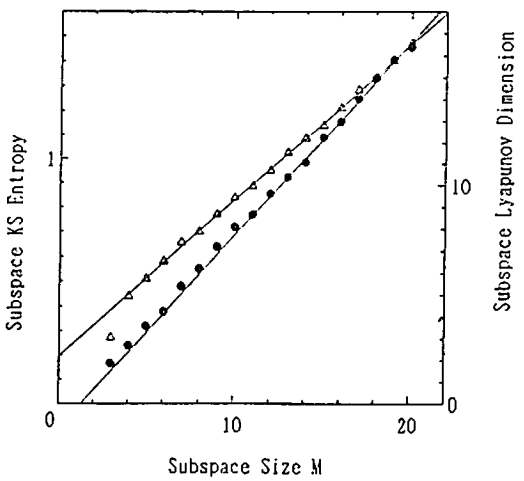


Fig. 9. $H(L)$(•) and $D_L(L)$(△) as a function of $L$. They are calculated from the subspace Lyapunov spectra for the logistic lattice with $a=1.9$, $\epsilon=0.4$ and $N=100$, starting from a random initial condition. The lines are drawn by the least square fit for $10<L<20$. The slopes are .75 (for KS entropy) and 7.2 (for Lyapunov dimension).

*) A one-dimensional case is explained here. The extension to higher dimensions is straightforward.

$L$. As is seen, it gives a good coincidence with the whole spectrum as $L$ is increased. The convergence is fast for positive exponents. For negative exponents, the convergence is rather slow, due to the boundary effect for the subspace. The subspace Lyapunov spectrum provides a simple way to estimate the density, such as Kolmogorov-Sinai entropy density and Lyapunov dimension density.

Subspace KS entropy $H(L)$ and Lyapunov dimension $D_L(L)$ are straightforwardly defined by replacing Lyapunov spectra by the subspace Lyapunov spectra. We propose here that

$$H(L)=hL+\text{const} \quad \text{and} \quad D_L(L)=d_L L+\text{const},$$

if the subspace size $L$ is large enough. This proposition provides a simple and efficient method to estimate the KS entropy and Lyapunov dimension densities. In Fig. 9, $H(L)$ and $D_L(L)$ are plotted as a function of $L$. The slopes of $H(L)$ and $D_L(L)$ in Fig. 9 are .75 and 7.2 respectively. On the other hand, $h\approx.74$ and $d_L\approx7.3$ from the calculation of whole $N$-dimensional Lyapunov spectrum. As is expected, our slopes give good estimates for these densities.

## § 5. Possible diagnosis of experimental data

The subspace Lyapunov spectra can be estimated from experimental data, if we adopt Takens-Packard embedding[28] and Sano-Sawada-Eckmann-Ruelle algorithm[29] for Lyapunov spectra. We propose the following algorithm for the diagnosis of experimental data of spatiotemporal chaos.*)

(i) From experimental data $x(r, t)$ in space $r$ and time $t$, measure the spatial and temporal correlations using mutual information, on the basis of the method in § 3. Here we assume that the correlation function decays fast enough to have a well-defined correlation length $\tau$ and $\xi$ (typically they decay exponentially as $\exp(-t/\tau)$ and $\exp(-r/\xi)$ for large $t$ and $r$).

(ii) From $x(r, t)$, we extract discrete sets of values $x_n(i)$ at discrete time and space with the interval $\tau_0$ and $\xi_0$. Here $\tau_0$ and $\xi_0$ should be smaller than, and the order of $\tau$ and $\xi$, respectively. Now we have a discrete set of $x_n(i)$ with $n=t/\tau_0$ and $i=r/\xi_0$.**)

(iii) Choose a subsystem with the size of $R=\xi_0 M$. Now we have a finite set of data $X_n\equiv x_n(j)$, $x_n(j+1)$, $\cdots$, $x_n(j+M-1)$. Following the idea of Packard et al. and Takens,[29] we reconstruct the dynamics of this subsystem by taking an embedding dimension $K$. Now we have $MK$-dimensional phase space $[X_n, X_{n+1}, \cdots, X_{n+M-1}]$.

(iv) Apply conventional methods to the above $MK$-dimensional time series: (a) algorithm to estimate the dimension (e.g., Grassberger-Procaccia algorithm[30]): (b) algorithm to estimate the Lyapunov spectrum (e.g., Sano-Sawada-Eckman-Ruelle algorithm[29]). Here we confine ourselves to the estimate of Lyapunov spectrum.***)

(v) Following the previous section and the above algorithm, we obtain

*) Here again, a one-dimensional case is used. The extension to higher dimensions is straightforward.

**) It is not yet resolved what the optimal choices for $\tau_0$ and $\xi_0$ are. As test choices, $\tau_0=\tau$ and $\xi_0=\xi$ may be recommended.

***) See Ref. 12) for the estimate of dimension density.

Lyapunov exponents for $MK$-dimensional dynamical systems; $\lambda_k(k=1, 2, \cdots, MK)$. Subspace Lyapunov dimension $d_L(K)$ and subspace Kolmogorov-Sinai entropy $h(k)$ are calculated from the spectrum.

(vi) Increase the number of spatial points $M$ fixing $K$, and carry out the same procedures (iv)~(v). We expect the following characterization:

(a) Plot $d_L(M)$ and check if it is fit by a linear increase form. If it is fitted, measure the slope (assume to be $\delta d_L$ for large $M$). The value $\delta d_L/\xi_0$ gives the Lyapunov dimension density.

(b) Plot $h(M)$ and check if it is fit by a linear form. If it is fitted, measure the slope (assume to be $\delta h$ for large $M$). The value $\delta h/\xi_0$ gives the Kolmogorov-Sinai entropy density.

(c) The scaled Lyapunov exponent $\lambda(x)\equiv\lambda_{MKx}$ fits on a single curve.

Since the estimate of negative Lyapunov exponents may be rather difficult, the Lyapunov dimension and the negative part of the scaled spectrum may be practically inaccurate. Still, we can hope to obtain KS entropy density and the positive part of scaled spectrum. The convergence of these two quantifiers distinguishes spatiotemporal chaos from random data.

## § 6. Sub-spacetime Lyapunov exponent

In the previous section we have assumed the spatial ergodicity. This assumption is valid to FDSTC, but it is also important to distinguish strongly chaotic spacetime region with weakly chaotic one. Here we introduce sub-spacetime Lyapunov exponents to study the spatiotemporal differentiation of chaos.

Take a subspace of the size $M=2L+1$ and calculate Lyapunov exponents only over finite time steps $T$. The exponents form the sub-spacetime Lyapunov spectrum. In our CML, the sub-spacetime Lyapunov exponent at time$=n$, site$=j$ is calculated by the products of Jacobi matrices for $[x_m(j-L), x_m(j-L+1), \cdots, x_m(j+L-1), x_m(j+L)]$ over $m=n, n+1, \cdots, n+T-1$. The boundary effect of amplification at $x_m(j-L)$ and $x_m(j+L)$ is again neglected.

To be specific, we calculate the product of the Jacobi matrices $J_n^{S(j-L,2L+1)}$ (Eq. (7))

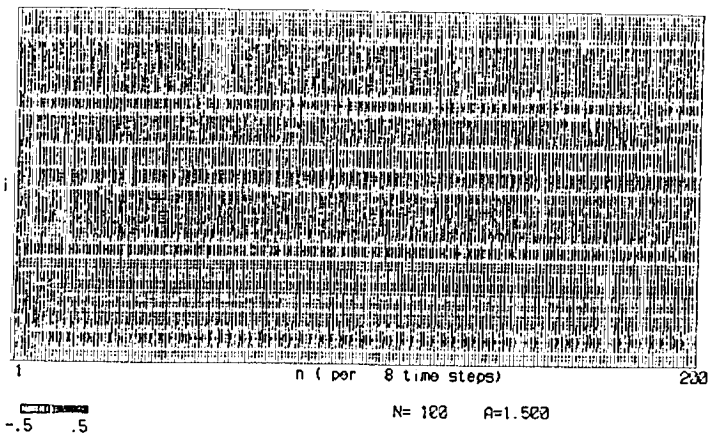


(a)

Fig. 10. (continued)

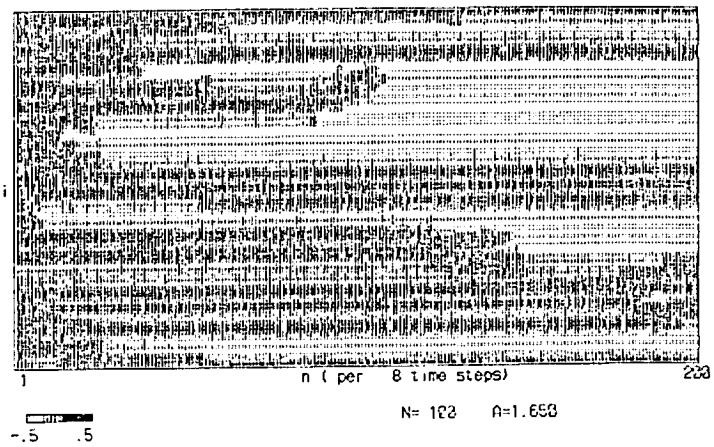


(b)

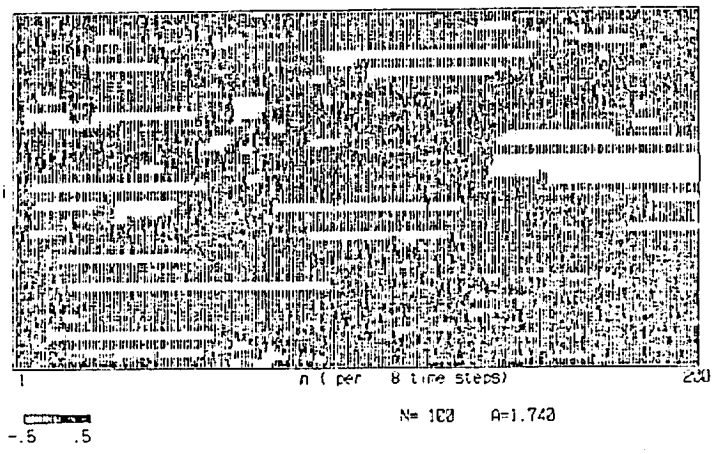


(c)

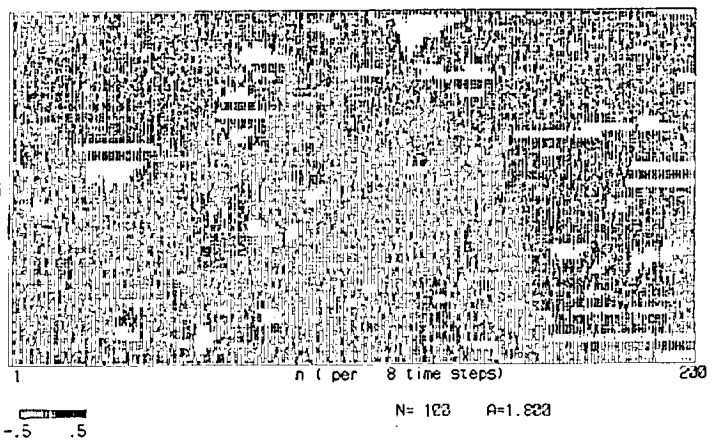


(d)

Fig. 10. Spacetime Lyapunov diagram: Sub-spacetime Lyapunov exponents with subspace size $M=3$ and sub-time length $k=8$ are calculated for the logistic lattice with $\epsilon=0.3$ and $N=100$. The gray-scale of the spacetime pixel represents the value of the exponent at the spacetime point. (a) $a=1.5$. (b) $a=1.65$. (c) $a=1.74$. (d) $a=1.8$.

over time steps $n=t, \cdots t+T$. Sub-spacetime Lyapunov exponents are given by the logarithms of the eigenvalues of the above product of Jacobi matrices.

In Fig. 10, maximal sub-spacetime Lyapunov exponents are plotted in spacetime with the use of subsystem size $L=1$ and $T=8$.

For frozen random pattern and pattern selection phases, spatial dependence of the exponents is clearly seen in Figs. 10(a) and (b). In spatiotemporal intermittency, we can distinguish burst and laminar regions clearly (see Fig. 10(c)). In FDSTC, fluctuation in spacetime is much smaller (Fig. 10(d)).

By sampling sub-spacetime Lyapunov exponents over the total lattice and many steps, we get the distribution of exponents $P(\lambda)$. The distribution provides a useful measure of statistical property of spatiotemporal chaos. In Fig. 11, the distribution of sub-spacetime Lyapunov exponents is shown.

In the frozen random pattern phase,[4] the distribution is widely scattered, representing the existence of different domain sizes with different strength of chaos

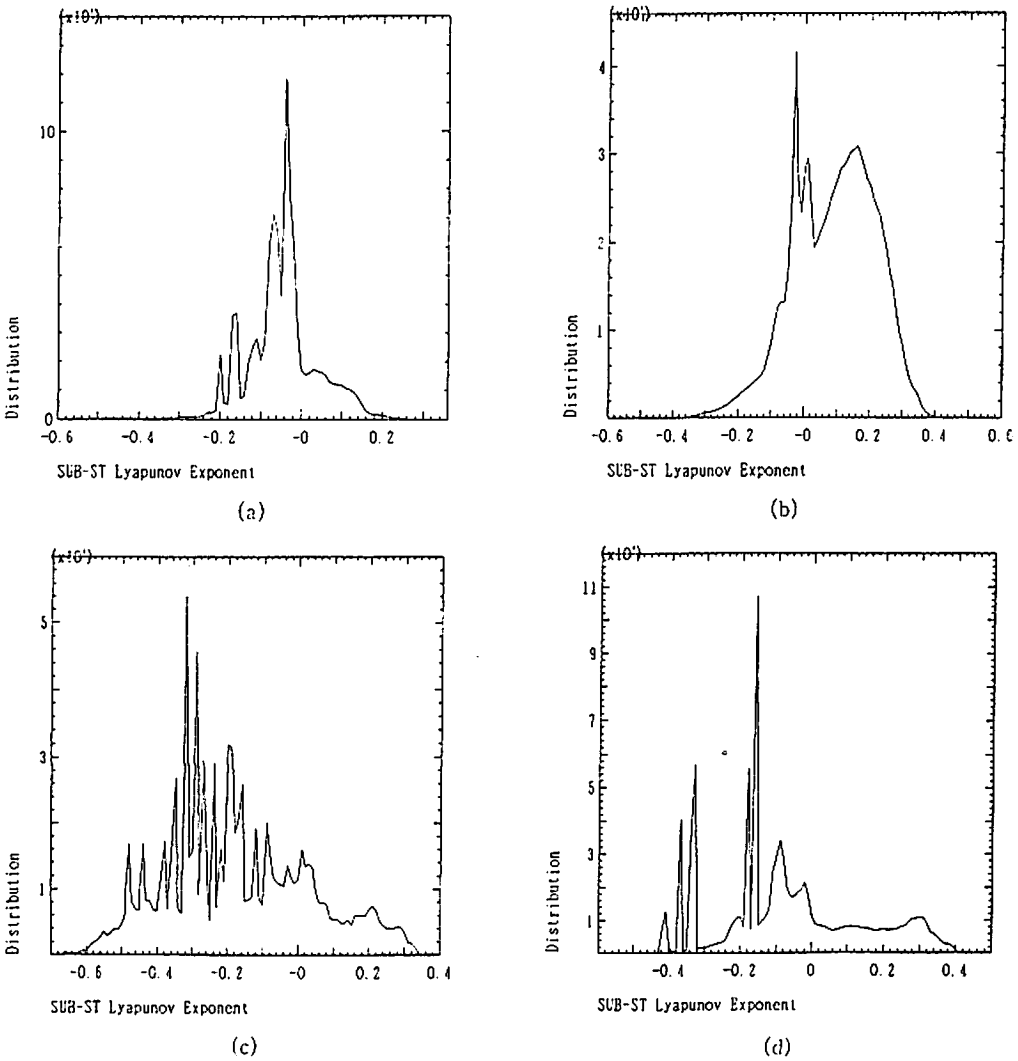


Fig. 11. (continued)

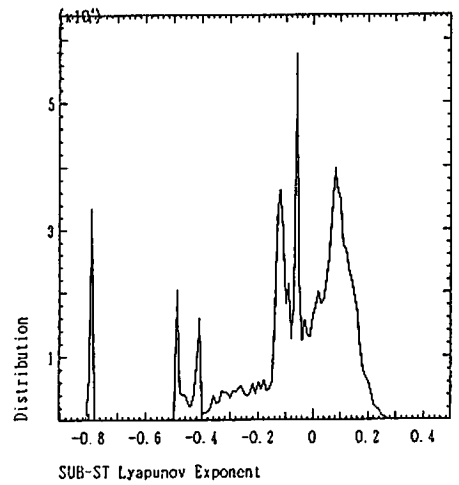


(e)

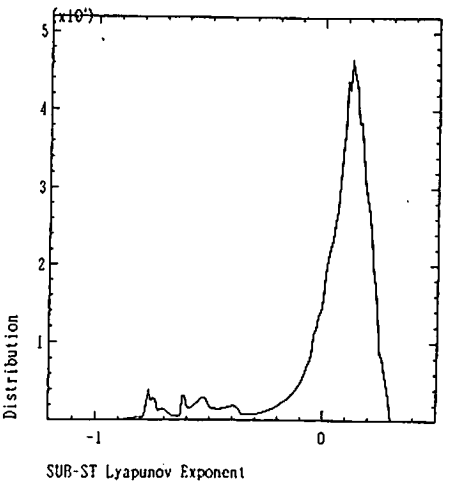


(f)

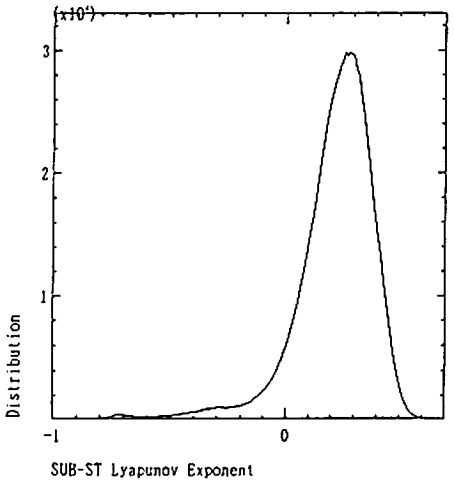


(g)

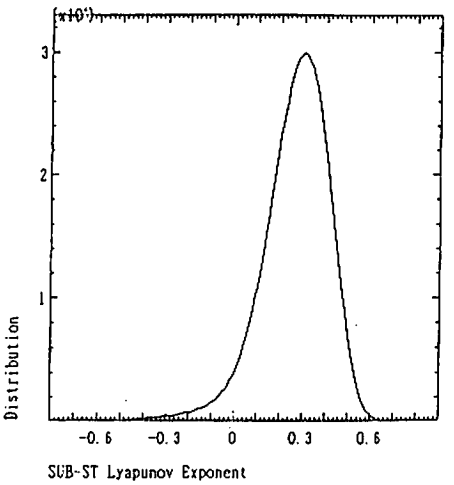


(h)

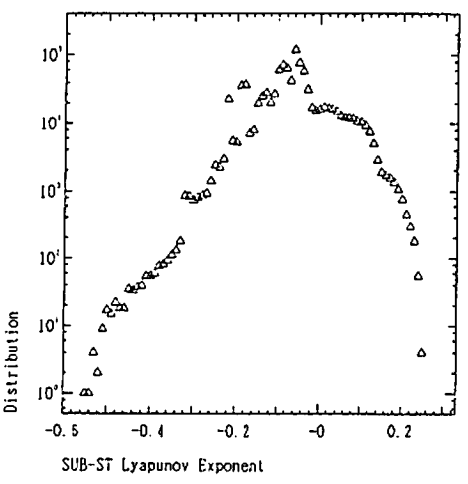


(a')

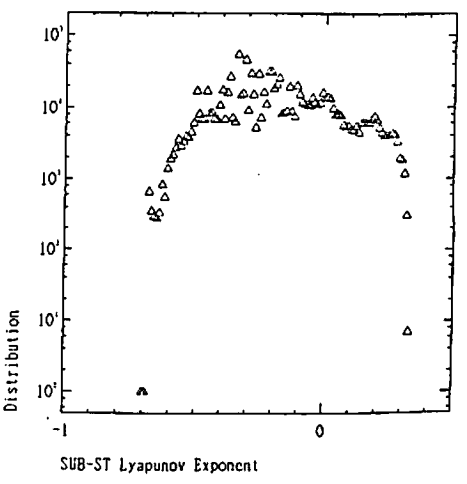


(c')

Fig. 11. (continued)

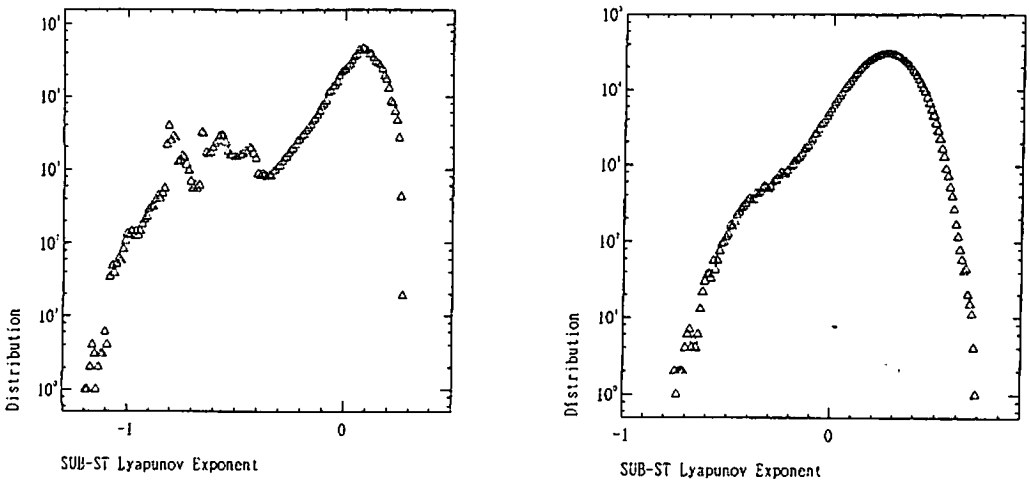


Fig. 11. Distribution of sub-spacetime Lyapunov exponents. Sub-spacetime Lyapunov exponents with subspace size $M=5$ and sub-time length $k=8$ are calculated for the lattice sites 10, 20, 30, ···, 100 and for 80000 steps per 8 steps. Totally $10\times10000$ exponents are obtained. From these data, histogram is sampled with the use of window size .01. Logistic lattice with $\epsilon=.3$ and $N=100$ from a random initial condition.

(a) $a=1.48$, (b) $a=1.54$, (c) $a=1.6$, (d) $a=1.66$, (e) $a=1.72$, (f) $a=1.74$, (g) $a=1.84$, (h) $a=1.94$.

For (a), (b) our systems are in frozen random phase, for (c), (d) in pattern selection phase, for (e), (f) in intermittency, and for (g), (h) it is in FTSTC.

Semilog plots are shown in (a'), (c'), (f'), and (h'), corresponding to (a), (c), (f) and (h) respectively.

(Figs. 11(a), (b), (a')). In the pattern selection phase, the distribution has few peaks (Figs. 11(c), (d), (c')). Note the peaks at negative values, showing the suppression of chaos[4] clearly. Peaks at positive exponents get lower as the nonlinearity $a$ is increased and the selection process proceeds.

At spatiotemporal intermittency, the distribution splits into two parts peaks at negative values and smooth distribution at positive values (Figs. 11(e), (f), (f')). This clear splitting means that the burst motion and laminar motion are well separated in our intermittency. As chaos is developed, the portion of the latter smooth distribution increases (Figs. 11(g), (h), (h')). The smooth distribution is not exactly Gaussian, but the tail of distribution decreases with $\exp(-\text{const}\times(\lambda-\lambda_0)^2)$. The width of the distribution becomes narrower with the increase of nonlinearity.

In future it will be of importance to apply the large-deviation-theory framework (Refs. 31)~35)) to our distribution of sub-spacetime Lyapunov exponents, in order to characterize the fluctuation in spacetime quantitatively.

## § 7. Self-consistent Perron-Frobenius operator

Is it possible to have a statistical mechanics formulation of spatiotemporal chaos? So far there are two approaches towards this direction.

The first approach is an inclusion of spatial degrees of freedom to the statistical mechanical theory of chaos. According to Refs. 32) and 33), chaos with one positive

Lyapunov exponent can be mapped to the statistical mechanics of a one-dimensional spin system. Then we may expect that a CML of $d$-dimensional lattice may be mapped into the statistical mechanics of a $(d+1)$-dimensional spin system. If this mapping is possible, we can construct Gibbs measure for our CML. We can also hope to map our phase transitions of pattern dynamics in CML onto the phase transition in a $(d+1)$-dimensional spin system. A cautionary comment here is that the interaction of this $(d+1)$-dimensional spin system should be strongly anisotropic, since the temporal direction of interaction and the coupling of spatial direction take completely different forms.

The first explicit construction of Gibbs measure for CML is carried out by Bunimovich and Sinai.[11] They have constructed the measure for a CML of an everywhere-expanding map with "almost"-diffusive coupling.

The second approach is the use of Perron-Frobenius (PF) operator.[13] In low-dimensional chaos, the PF operator has been useful for the study of the statistical mechanics. Since the PF operator is applied to the probability measure $\rho(x(1), x(2), \cdots, x(N))$ for the whole $N$-dimensional phase space, it is practically intractable for our CML with (large) $N$ degrees of freedom.

On the other hand, the heat-bath picture is valid, especially in FDSTC, as has been discussed in previous sections. Our dynamics in a given subspace can be approximated by the dynamics of the subspace and the stochastic process at the boundary. To determine the nature of stochasticity, we adopt the self-consistent approximation here. The strategy is as follows: By applying the PF operator to a subspace with a noisy boundary, we obtain the measure for the subspace. The noise at the boundary is determined by the measure self-consistently.*)

The PF operator for the entire dynamical system is given by[32),34),36)]

$$H^{PF}\rho(x(0), \cdots, x(N-1)) = \sum_{y(i)=\text{preimages}} \frac{\rho(y(0), \cdots, y(N-1))}{J(y(0), \cdots, y(N-1))}, \tag{8}$$

where the sum takes over all possible sets of $(y(i))$, preimages of $x(i)$ (i.e., $y(i) \to x(i)$ by the map (1)). $J(y(0), \cdots, y(N-1))$ is the Jacobian of the CML transformation (1).

The preimages of our system are easily calculated as in Refs. 5) and 13). First we introduce the inverse of the tridiagonal diffusion matrix $D_{i,j} = (1-\epsilon)\delta_{i,j} + (\epsilon/2)(\delta_{i,j+1} + \delta_{i,j-1})$. It is given by

$$x'(j) = \sum_{l=0}^{N-1} D_{jl}^{-1} x(l) \equiv \sum_{l=0}^{N-1} (1/N) \sum_{k=0}^{N-1} \frac{\exp(2ik\pi(l-j)/N)}{1-2\epsilon\sin^2(k\pi/N)} x(l). \tag{9}$$

The preimages in Eq. (8) are given by

$$y(i) = f^{-1}(x'(j)) = f^{-1}(\sum_l D_{jl}^{-1} x(l)), \tag{10}$$

where $f^{-1}(x)$ is inverse functions of $f(x)$ (for the logistic map it is given by $\pm\sqrt{(1-x)/a}$). Using the chain rule, we get the following expression for the entire PF operator:

*) Here we discuss 1-dimensional lattices with diffusive coupling. Extensions of our formulation to the open-flow CML model,[7] and higher-dimensional lattices[5] are straightforward.

$$H^{PF}\rho(x(1), x(2), \cdots, x(N))=(\det D)^{-1}\sum_{y(1),\cdots,y(N)}\frac{\rho(y(1),\cdots,y(N))}{\prod_{j=1}^{N}|f'(y(j))|}, \tag{11}$$

where $\sum_{y(1),\cdots,y(N)}$ runs over all possible solutions of Eq. (10).

Projection onto the $k$-dimensional subspace $(x(1), x(2), \cdots, x(k))$ is carried out by integrating out other lattice points than 1, 2, $\cdots$, $k$:

$$\rho(x(1), x(2), \cdots, x(k))$$

$$=\int\cdots\int dx(0)dx(k+1)dx(k+2)\cdots dx(N-1)\rho(x(0), x(1), \cdots, x(N-1)).$$

In order to integrate out Eq. (11) by $dx(0)dx(k+1)dx(k+2)\cdots dx(N-1)$, we need the information at the boundary at 0 and $k+1$. For this, we have to introduce the following conditional probability:

$$P(y(2), y(3), \cdots, y(k)|y(k+1))$$

$$=\rho(y(2), y(3), \cdots, y(k), y(k+1))/\rho(y(2), y(3), \cdots, y(k)). \tag{12}$$

Neglecting spatial correlation longer than $k$ in $\rho(x(0), \cdots, x(N-1))$, we obtain the following expression for subspace distribution function:

$$H^{SPF}\rho(x(1), x(2), \cdots, x(k))=(\det D'(k))^{-1}\iint\sum_{y(1),\cdots,y(s)}dy(0)dy(k+1)$$

$$\frac{\rho(y(1), \cdots, y(k))P(y(2), y(3), \cdots, y(k)|y(k+1))P(y(1), y(2), \cdots, y(k-1)|y(0))}{\prod_{j=1}^{k}|f'(y(j))|}. \tag{13}$$

The preimages $(y(1), y(2), \cdots, y(k))$ are given by the solution of

$$y(j)=f^{-1}(D'^{-1}_{j,l}(k)x_l-(\epsilon/2)(f(y(0))\delta_{j,1}+f(y(k+1))\delta_{j,k})). \tag{14}$$

The matrix $D'(k)$ is the $k$-dimensional diffusion matrix $D_{ij}$ of size $k$ without a periodic boundary (i.e., $(1-\epsilon)\delta_{i,j}+(\epsilon/2)(\delta_{i+1,j}+\delta_{i-1,j})$).

The above equation is easily interpreted as the PF operator for the CML of size $k$ with the boundary at $x(0)=y(0)$ and $x(k+1)=y(k+1)$. The probability that $x(0)$ and $x(k+1)$ take $y(0)$ and $y(k+1)$ is calculated by $\rho(y(0), y(1), \cdots, y(k-1))$ and $\rho(y(2), y(3), \cdots, y(k+1))$ *self-consistently* from our $k$-dimensional probability distribution function.

The projected invariant measure $\rho^*(x(1), \cdots, x(k))$ onto a $k$-dimensional space is obtained as the fixed point function of the above operator.

For $k=1$ (one-body approximation), the self-consistent PF(SPF) operator is given by

$$H^{SPF}\rho(x)=(1-\epsilon)^{-1}\iint_{\sum_{y=f^{-1}((x-\epsilon/2(y_0+y_2)))/(1-\epsilon))}}\frac{\rho(y)\rho(y_0)\rho(y_2)}{|f'(y)|}dy_0dy_2, \tag{15}$$

where the sum over preimages $y$ are given by the solutions of $y=f^{-1}((x-\epsilon/2(y_0+y_2))/(1-\epsilon))$.

For $k=2$ (two-dody approximation), it is given by

$$H^{\mathrm{SPF}}\rho(x_1, x_2)=((1-\epsilon)^2-(\epsilon/2)^2)^{-1}\iint\sum_{y1,y2}\frac{\rho(y_1, y_2)\rho(y_0, y_1)\rho(y_2, y_3)}{\rho(y_1)\rho(y_2)|f'(y_1)f'(y_2)|}dy_0dy_3\,, \quad (16)$$

where $\rho(y_2)=\int\rho(y_1, y_2)dy_1$ and the preimages $(y_1, y_1)$ are given by the solutions of

$$f(y_1)=(1-\epsilon)x_1+\epsilon(f(x_2)+y_0)/2\,;\ f(y_2)=(1-\epsilon)x_2+\epsilon(f(x_1)+y_3)/2\,.$$

Extensions to a larger $k$-dimensional subspace are quite straightforward. In the following, we briefly present some applications of 1-body and 2-body SPF to phase transitions in CML.

Let us discuss the spatiotemporal intermittency at the period-3 window in our logistic lattice ($a=1.752$) (§ 2). At $\epsilon\approx.0008$, spatiotemporal intermittency phase transition occurs, as is discussed in § 2. By our SPF operator, the transition occurs at $\epsilon\approx.0008$. Even in this one-body approximation the coincidence is within 10%.

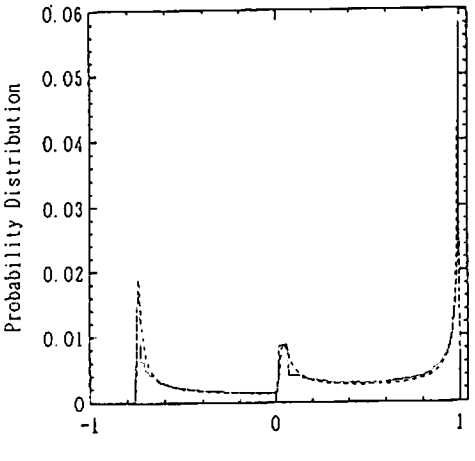


Fig. 12. One-body distribution function of $\rho(x)$. The solid line gives a 1-body distribution function obtained from numerical integration of our self-consistent approximation, while the dotted line gives that obtained from a direct simulation of (1). For the calculation of distribution, 320 mesh points are used for the interval $(-1, 1.1)$ ($\Delta x=2.1/320$). The logistic lattice with $a=1.752$ and $\epsilon=.002$. For the direct simulation, data are sampled over 30000 time steps after 10000 transients, over the total lattice points with the size $N=1000$, and starting from a random initial condition.

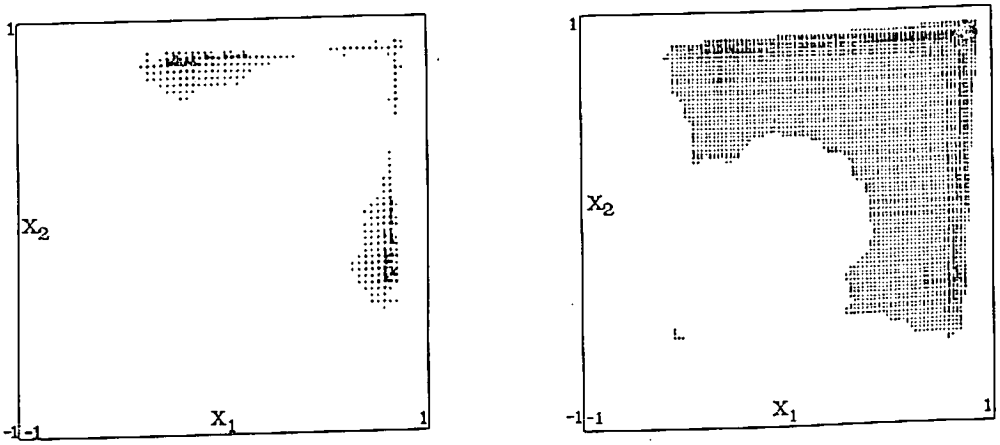


Fig. 13. Two-body distribution function of $\rho(x_1, x_2)$, obtained from the numerical integration of Eq. (16). For integration 64 meshes are used for $(-1, 1)$ ($\Delta x=2/64$). In the figure, a side of a square is proportional to $\rho(x_1, x_2)$ at the corresponding site. (a) $a=1.84$, $\epsilon=.1$ (the maximum of $\rho(x_1, x_2)(\Delta x)^2$ is 0.0061; the corresponding pixel is left blank if $\rho(x_1, x_2)(\Delta x)^2<0.001$). (b) $a=1.9$, $\epsilon=.1$ (the maximum of $\rho(x_1, x_2)(\Delta x)^2$ is 0.0015; the pixel is left blank if $\rho(x_1, x_2)(\Delta x)^2<0.0001$).

The invariant measure $\rho(x)$ vanishes for $x \in I_j$ for $\epsilon < \epsilon_c$. For $\epsilon > \epsilon_c$, $\rho(x)$ is a continuous measure. The invariant measures obtained by our SPF and by direct simulation are plotted in Fig. 12. As is seen, the above one-body approximation is fairly accurate in FDSTC.

The next example is the phase transition with pattern dynamics in our logistic lattice (1).[4] To see the ordered pattern with a domain size of $l$, we need at least $l$-dimensional distribution function. The simplest transition is that from a zigzag pattern ($l=2$) to a turbulent state at $\epsilon=.1$. In Fig. 13, two-point distribution functions $\rho(x(1), x(2))$ are shown. We can see a transition from a zigzag state to a turbulent state. This kind of transition is seen even in a coupled-logistic map of two elements (Ref. 38)). In the treatment here, the effect of other sites than the 2-lattice-point subspace is included as a self-consistent heat bath.

Besides theoretical aspects, our SPF has numerical merits. The convergence to a fixed point function here is exponential and quite rapid (in our examples within 10-30 steps), while in the direct simulation, the covergence is $1/\sqrt{time}$ and requires more than 10000 steps.

If we take a larger subspace, it is expected that our approximation of the measure would be better. Since the spatial correlation decays exponentially in FDSTC, our SPF is expected to be accurate if the subsystem size is larger than the correlation length.

Once we get the distribution $\rho(x(1), x(2), \cdots, x(k))$, it is possible to calculate the mutual information in space, and estimate the subspace Lyapunov exponents and Kolmogorov-Sinai entropy density with the use of subspace Jacobi matrix (Eq. (7)).

The two-point distribution $P(x(1), x(k))$ and one-point distribution $p(x)$ in Eq. (5) are straightforwardly obtained by the integrations as

$$P(x(1), x(k)) = \int \cdots \int \rho(x(1), \cdots, x(k)) dx(2) dx(3) \cdots dx(k-1).$$

Spatial mutual information is directly obtained from this probability distribution. Spatial patch entropy is calculated directly as

$$-\int \rho(x(1), \cdots, x(k)) \log \rho(x(1), \cdots, x(k)) dx(1) \cdots dx(k).$$

## § 8. Summary and discussion

In the present paper we have discussed thermodynamics of spatiotemporal chaos, with the emphasis on the fully developed spatiotemporal chaos (FDSTC). First, stability of FDSTC is confirmed. Windows of local dynamical systems are destroyed by spatiotemporal intermittency. It is found that the spatiotemporal intermittency here belongs to type-II supertransient turbulence. In type-II supertransients, the length of transients diverges exponentially with system size; $\exp(rN)$. The coefficient $r$ increases with $\epsilon$ as $r \propto (\epsilon - \epsilon_c)^{\gamma}$. The quasistationary measure exists in the transient regime. FDSTC is sustained for large $N$ by this supertransient turbulence.

In FDSTC, spatial and temporal correlations decay exponentially, as are measured by mutual information. We can adopt the heat-bath picture; approximate replacement of our dynamics by local chaos in a subspace and the heat bath from boundaries. When this heat-bath picture is valid, we can estimate thermodynamical densities from subspace Lyapunov exponents. An algorithm for the analysis of experimental data is proposed on the basis of the embedding and subspace Lyapunov exponent.

Sub-spacetime Lyapunov exponents are introduced. By the exponents, one can distinguish chaotic and laminar regions in spacetime. Distribution of the exponents gives a statistical measure of the fluctuation of chaos in spacetime. In spatiotemporal intermittency, for example, the separation of chaotic burst and ordered motion is clearly seen in this distribution.

As a step towards theoretical analysis, self-consistent Perron-Frobenius operator is studied. It gives a fairly accurate approximation for the invariant measure.

Here we note that this self-consistent formulation is not a mean-field theory. The mean-field theory in the original sense should be derived as a global coupling model for our lattice system, i.e., $x_{n+1}(i)=(1-\epsilon)f(x_n(i))+(\epsilon/N)\sum_j f(x_n(j))$. See Ref. 17) for three phases in this globally coupled map corresponding to the pattern dynamics of our short-ranged lattice systems.

Through thermodynamics of spatiotemporal chaos, we hope to find possible relations among quantifiers, e.g., correlation length and time, KS entropy density, Lyapunov spectrum, and so on.

In chaos with a single positive Lyapunov exponent, it is argued that mutual information and Lyapunov exponent are related by $I'(t)\approx I^0-\lambda_{\max}t$ for small $t$.[26] For larger $t$, the decay of mutual information is related with the diffusion process in phase space. So far, no relation of this diffusion with Lyapunov exponent is known.

In spatiotemporal chaos, no explicit relations are known even between mutual information and Lyapunov spectra. If the diffusion process in phase space is related with KS entropy density $h$, the correlation time $\tau(I'(t)\approx\exp(-t/\tau))$ can be related with $h$. In numerical data, $\tau$ and $h$ are strongly correlated in FDSTC, but the proportionality between the two does not hold.

In FDSTC, our system is approximated by the dynamics of $(N/\xi)$ independent subunits. If chaos in a single subunit were characterized just by the maximal Lyapunov exponent $\lambda_{\max}$, KS entropy density $h$ would be proportional to $\lambda_{\max}/\xi$. In numerical data, this proportionality does not hold correctly, but can work as a first approximation.

Construction of thermodynamics of spatiotemporal chaos and search for relations among quantifiers still remain to be important problems in future.

## Acknowledgements

It is my great pleasure to dedicate the present paper to Professor Mori on the occasion of his retirement from Kyushu University. It was 10 years ago that I first met Professor Mori, when we were working on the adiabatic elimination in stochastic systems. Since then I have always been indebted to Professor Mori for his continual encouragements, and useful discussions.

I would also like to thank J. P. Crutchfield, M. Casdagli, N. H. Packard, H. Gutowitz, J. D. Farmer, G. Mayer-Kress, M. H. Jensen, D. K. Umberger, and M. Sano for useful discussions.

## References

1) (a) K. Kaneko, Prog. Theor. Phys. 72 (1984), 480.
(b) K. Kaneko, Prog. Theor. Phys. 74 (1985), 1033.
(c) K. Kaneko, in *Dynamical Problems in Soliton Systems*, ed. S. Takeno (Springer, 1985), p.272.
2) K. Kaneko, Ph. D. Thesis, *Collapse of Tori and Genesis of Chaos in Dissipative Systems*, 1983 (enlarged version is published by World Sci. Pub., 1986).
3) K. Kaneko, Physica 23D (1986), 436.
4) K. Kaneko, Physica 34D (1989), 1 ; Europhys. Lett. 6 (1988), 193 ; Phys. Lett. 125A (1987), 25.
5) K. Kaneko, Physica 37D (1989), 60.
6) J. P. Crutchfield and K. Kaneko, "Phenomenology of Spatiotemporal Chaos", in *Directions in Chaos* (World Scientific, 1987), p. 272.
7) K. Kaneko, Phys. Lett. 111A (1985), 321.
R. J. Deissler and K. Kaneko, Phys. Lett. 119A (1987), 397.
8) For CML see also ;
R. E. Deissler, Phys. Lett. 120A (1984), 334.
I. Waller and R. Kapral, Phys. Rev. 30A (1984), 2047.
R. Kapral, Phys. Rev. 31A (1985), 3868.
G. L. Oppo and R. Kapral, Phys. Rev. A33 (1986), 4219; A36 (1987), 5820; Physica 23D (1986), 455.
R. Kapral, G. L. Oppo and D. B. Brown, Physica 147A (1987), 77.
K. Kaneko, in *Dynamical Systems and Singular Phenomena*, ed. G. Ikegami (World Sci., 1987).
Y. Aizawa, Prog. Theor. Phys. 72 (1984), 662.
T. Yamada and H. Fujisaka, Prog. Theor. Phys. 72 (1984), 885 ; 74 (1985), 918.
T. Bohr et al., Phys. Rev. Lett. 58 (1987), 2155.
F. Kaspar and H. G. Schuster, Phys. Lett. 113A (1986), 451; Phys. Rev. A36 (1987), 842.
P. Alstrom and R. K. Ritala, Phys. Rev. 35A (1987), 300.
S. Coppersmith, Phys. Rev. 38A (1988), 375.
K. Aoki and N. Mugibayashi, Phys. Lett. 128A (1988), 349.
P. Grassberger, Preprint (1987) "Lumped and Distributed Dynamical Systems".
K. Kaneko and T. Konishi, J. Phys. Soc. Jpn. 56 (1987) 2993 ; Phys. Rev. A40 (1989), 6130.
H. Kanz and P. Grassberger, J. of Phys. A21 (1988), L127.
I. Tsuda and H. Shimizu, in *Complex Systems—Operational Approaches*, ed H. Haken (Springer 1985).
H. Chate and P. Manneville, CR Acad. Sci. Paris 304 (1987), 609 ; J. Stat. Phys. 56 (1989), 357.
M. Rotenberg, Physica 30D (1988), 192.
J. Brindley and R. M. Everson, Phys. Lett. A134 (1989), 229.
I. S. Aronson, A. V. Gaponov-Grekhov and M. I. Rabinovich, Physica 33D (1988), 1.
Y. Oono and S. Puri, Phys. Rev. Lett. 58 (1986), 836; Phys. Rev. 38A (1988), 1542.
M. H. Jensen, Phys. Rev. Lett. 62 (1989), 1361; to appear in Physica D.
H. Nishimori and T. Nukii, J. Phys. Soc. Jpn. 58 (1989), 563.
P. Hadley and K. Wiesenfeld, Phys. Rev. Lett. 62 (1989), 1335.
T. Bohr and O. B Christensen, Phys. Rev. Lett. 63 (1989), 2161.
Y. Oono and A. Shinozaki, Forma (in press).
G. Grinstein, Preprint (1988).
D. Rand and T. Bohr, Preprint (1988).
L. A. Bunimovich, A. Lambert and R. Lima, Preprint (1989).
S. Isola, A. Politi, S. Ruffo and A. Torcini, Phys. Lett. 143A(1990), 365.
F. Bagnoli et al., Preprint (1989).
C. Bennet et al., Preprint (1989).

9) J. D. Keeler and J. D. Farmer, Physica 23D (1986), 413.
H. Chate and P. Manneville, Phys. Rev. A38 (1988), 4351; Europhys. Lett. 6 (1988), 50 ; Physica 32D (1988), 409.
10) J. P. Crutchfield and K. Kaneko, Phys. Rev. Lett. 60 (1988), 2715.
11) L. A. Bunimovich and Ya. G. Sinai, Nonlinearity 1 (1989), 491.
12) G. Mayer-Kress and K. Kaneko, J. Stat. Phys. 54 (1989), 1489.
13) K. Kaneko, Phys. Lett. 139A (1989), 47.
14) For the analysis of spatiotemporal intermittency by the self-consistent Perron-Frobenius operator see J. M. Houlrik, I. Webman and M. H. Jensen, Preprint NORDITA-89/46.
15) K. Kaneko "Simulating Physics with Coupled Map Lattices—Pattern Dynamics, Information Flow, and Thermodynamics of Spatiotemporal Chaos" in *Formation, Dynamics, and Statistics of Patterns*, ed. K. Kawasaki, A. Onuki and M. Suzuki (World Sci., 1990).
16) K. Kaneko, "Climbing Up Dynamical Hierarchy", in *Chaotic Hierarchy*, ed. G. Baier and M. Klien (World Sci., 1990).
17) K. Kaneko, Phys. Rev. Lett. 63 (1989), 219; "Clustering, Coding, Switching, Hierarchical Ordering in Globally Coupled Chaotic Systems", Physica D (1990), (in press).
18) *Spatiotemporal Coherence and Chaos in Physical Systems*, Physica 23D (1986), ed. A. R. Bishop, G. Grüner and B. Nicolaenko.
19) For spatiotemporal chaos, see also:
B. Nicolaenko, Nucl. Phys. B (Suppl.) 2 (1987), 453.
W. Y. Tam et al., Phys. Rev. Lett. 61 (1988), 2163.
K. Otsuka and K. Ikeda, Phys. Rev. Lett. 59 (1987), 191.
D. K. Umberger, C. Grebogi and E. Ott, Phys. Rev. A39 (1989), 4835.
A. V. Gaponov-Grekhov and M. I. Rabinovich, Sov. Phys.-Usp. 30 (1987), 433.
20) For spatiotemporal chaos in Josephson junction array, see, e.g.,
R. Mehrotra and S. R. Shenoy, Europhys. Lett. 9 (1989), 11.
L. E. Guerrero and M. Octavio, Phys. Rev. A40 (1989), 3371.
21) See for some experiments on spatiotemporal intermittency;
S. Ciliberto and P. Bigazzi, Phys. Rev. Lett. 60 (1988), 286.
S. Nasuno, M. Sano and Y. Sawada, in *Cooperative Dynamics in Complex Systems*, ed. H. Takayama (Springer, 1989).
F. Daviaud, M. Dubois and P. Berge, Europhys. Lett. 9 (1989), 441.
J. Gollub and R. Ramshankar, to appear in *New Perspectives in Turbulence*, ed. S. Orszag and L. Sirovich (Springer).
22) L. D. Landau and E. M. Lifshitz, *Fluid Mechanics* (Pergamon, London, 1959), chap. 3.
23) D. Ruelle and F. Takens, Comm. Math. Phys. 20 (1971), 167; 23 (1971), 343.
24) O. E. Rössler, Phys. Lett. 71A (1979), 155 ; in *Lecture Notes in Applied* Math. 17 (1979), p. 141.
See also O. E. Rössler, Z. Naturforsch. 38a (1983), 788.
25) T. Li and J. A. Yorke, Amer. Math. Monthly 82 (1975), 985.
26) R. Shaw, Z. Naturforsh. 36a (1981), 80.
27) J. Kaplan and J. A. Yorke, in *Springer Lecture Notes in Mathematics* 730 (1979), p. 204.
28) N. H. Packard et al., Phys. Rev. Lett. 45 (1980), 712.
F. Takens, in *Dynamical Systems and Turbulence* ed. D. Rand and L-S. Young (Springer, 1981).
29) M. Sano and Y. Sawada, Phys. Rev. Lett. 55 (1985), 1082.
J. P. Eckmann and D. Ruelle, Rev. Mod. Phys. 57 (1985), 617.
30) P. Grassberger and I. Procaccia, Physica 13D (1984), 34.
31) R. S. Ellis, Entropy, *Large Deviations and Statistical Mechanics* (Springer Verlag, 1985).
32) R. Bowen and D. Ruelle, Inventiones Math. 29 (1975), 181.
D. Ruelle, *Thermodynamic Formalism* (Addison Wesley, Reading, MA, 1978).
33) M. Gutzwiller, Physica 5D (1982), 183.
34) Y. Oono, Prog. Theor. Phys. 60 (1978), 1944.
Y. Oono and Y. Takahashi, Prog. Theor. Phys 63 (1980), 1804.
35) H. Fujisaka, Prog. Theor. Phys. 70 (1983), 1264.

M. Sano, S. Sato and Y. Sawada, Prog. Theor. Phys. 76 (1988), 945
J.-P. Eckmann and I. Procaccia, Phys. Rev. A34 (1986), 659.
H. Mori, H. Hata, T. Horita and T. Kobayashi, Prog. Theor. Phys. Suppl. No. 99 (1989), 1.
36) H. Mori, B-C. So and T. Ose, Prog. Theor. Phys. 66 (1981), 1266.
37) H. A. Gutowitz, J. D. Victor and B. W. Knight, Physica 29D (1987), 18.
38) K. Kaneko, Prog. Theor. Phys. 69 (1983), 1477.
39) H. A. Gutowitz and J. D. Victor, Complex Systems 1 (1987), 57; J. Stat. Phys. 54 (1989), 495.